J. Mietzner and P. A. Hoeher, “Distributed space-time codes for cooperative wireless networks in the presence of different propagation delays and path losses,” in *Proc. 3rd IEEE Sensor Array and Multichannel Signal Processing Workshop (SAM 2004)*, Sitges, Barcelona, Spain, July 2005, pp. .

Distributed Space-Time Codes for Cooperative Wireless Networks in the Presence of Different Propagation Delays and Path Losses

Jan Mietzner and Peter A. Hoeher
Information and Coding Theory Lab (ICT), Faculty of Engineering, University of Kiel, Kaiserstrasse 2, D-24143 Kiel, Germany
WWW: `www-ict.tf.uni-kiel.de` E-mail: `{jm,ph}@tf.uni-kiel.de`

Abstract— **The application of a distributed space-time coding scheme in a simulcast network is considered. A key challenge is addressed which is particularly crucial in the downlink: Since the distances between the individual transmitting nodes and the receiving node are typically different, the transmitted signals are subject to different propagation delays and to different path losses. The influence of these effects on the system performance is investigated for the example of a specific space-time coding scheme, based on simulative and analytical results. Specifically, the issue of equalization/detection at the receiver is addressed, and a joint equalizer/detector algorithm of practicable complexity is proposed for large relative propagation delays.**

Index Terms—**Wireless communications, cooperative networks, distributed space-time coding techniques.**

I. INTRODUCTION

WIRELESS communication systems with multiple antennas have recently attracted considerable interest [1]. This is because the performance of a wireless system is often limited by fading and may be significantly improved by exploiting some sort of diversity, for example, *spatial* diversity.

Spatial diversity results from the fact that the individual transmission paths from the transmit (Tx) antennas to the receive (Rx) antennas are likely to fade independently. *Space-time codes (STCs)* for multiple antenna systems yield an additional diversity and/or coding gain compared to a (1x1)-system with only a single antenna at either end of the link. With STCs, multiple antennas are only required at the transmitter, whereas multiple Rx antennas are optional.

The concept of multiple antennas may be transferred to *cooperative* wireless networks, where multiple (single-antenna) nodes share their antennas by using a *distributed* STC scheme. Just as in a conventional multiple-antenna system, the nodes may thus exploit spatial diversity ('cooperative diversity'). The idea of cooperating network nodes is gaining more and more attention in the literature, because cooperating nodes build the basis of any ad-hoc network. In addition, cooperative diversity promises considerable benefits also for other types of networks, such as cellular networks and sensor networks. Examples for cooperative wireless networks include simulcast networks (e.g. [2]) and relay-assisted networks (e.g. [3]).

Simulcast networks are, for example, employed for broadcasting or for paging applications, i.e., either when many mobile users are to be served simultaneously or when the position of a single desired user is unknown. Conventionally, several serving nodes simultaneously transmit the same signal using the same carrier frequency. Simulcasting may, for example, be applied in satellite-aided systems (cf. Fig. 1 (a)). In cellular systems, simulcasting may be used in areas that are served by multiple base stations, in order to reduce the probability of shadowing (synchronized base stations are already deployed in practice). However, conventional simulcasting does not yield a diversity gain [2]. In relay-assisted networks, the transmitted signal of a certain source node, e.g., a mobile station, is received by several relay nodes, which then forward the signal to a certain destination node. Relaying may either be performed by fixed stations or by other mobile stations.

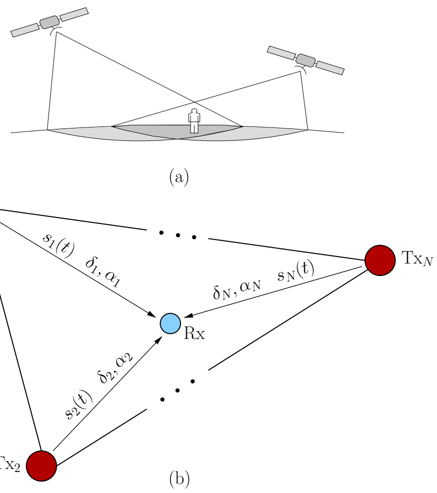

Fig. 1. (a) Satellite-aided system with a mobile user having intervisibility with two satellites (b) Simulcast network with N Tx nodes and one Rx node (downlink).

In this paper, the application of a distributed STC scheme in a simulcast network is addressed. An example for a simulcast network with N Tx nodes and one Rx node is given in Fig. 1 (b). If all nodes employ a single antenna and if no shadowing occurs, a diversity degree of N may be achieved by means of an appropriate distributed STC scheme for N Tx antennas. For instance, an orthogonal space-time block code (OSTBC) [4],[5] may be employed. On the one hand, OSTBCs achieve full diversity in terms of the number of Tx nodes. On the other hand, they have another desirable property [3]: If *any* subset of $n < N$ Tx nodes is completely obstructed due to shadowing, OSTBCs still grant a diversity degree of $(N-n)$. A drawback of these STC schemes is, however, that for $N > 2$ no OSTBC exists with a temporal rate of one [6]. For $N = 2$, the well-known Alamouti scheme [4] provides a temporal rate of one; therefore the focus will be on this scheme here. Even if there are more than two Tx nodes available, it may still be useful to employ the Alamouti scheme – in conjunction with a *selection diversity* scheme [7] choosing those two nodes that are associated with the best transmission paths toward the Rx node, e.g., in terms of average signal-to-noise ratio (SNR).

Within the scope of this paper, a key challenge is considered that is particularly crucial in the *downlink* of a simulcast network: As the distances between the individual Tx nodes and the Rx node are typically different, the transmitted signals $s_i(t)$, $i = 1, ..., N$, are subject to different propagation delays δ_i and to different average path gains α_i (cf. Fig. 1 (b)), provided that no counter measures are applied. Different path gains α_i may also be caused by shadowing. Since these effects are due to the distributed nature of the STC scheme under consideration, they are usually not addressed in the standard literature on STCs.

The paper is organized as follows: The system model under consideration is introduced in Section II. The impact of different average path gains α_i on the system performance is studied in Section III, based on analytical and simulative results. In Section IV it is shown that different propagation delays δ_i cause intersymbol interference (ISI). A joint equalizer/detector algorithm for the Alamouti scheme in the presence of ISI proposed in an earlier work [8] is briefly recapitulated, and the influence of different propagation delays is investigated. Moreover, the case of large relative propagation delays is considered, which may, for example, occur in a satellite-aided system. It is shown that the concept of 'sparse' wireless channels [9],[10] can be exploited to derive an equalizer/detector algorithm of comparably low complexity for this scenario.

II. System Model

Throughout this paper, the equivalent complex baseband representation is used. It is assumed that the Tx nodes are perfectly synchronized in time and in frequency. In order to counteract the different propagation delays δ_i, the Tx nodes may apply some sort of *timing-advance (TA)* protocol [11, Ch. 8.3]. For this purpose, each delay δ_i must be known at the corresponding Tx node Tx_i. The Tx nodes may then adjust the timing of their transmitted signals accordingly. Similarly, in order to counteract the different average path gains α_i, the Tx nodes may apply some sort of *link-adaptation (LA)* protocol [11, Ch. 8.10] to adapt their average transmission powers.

In the sequel, focus is on a distributed Alamouti scheme, where the two Tx nodes and the Rx node each employ a single antenna. The Alamouti scheme [4] was designed for quasi-static frequency-flat fading channels. In the equivalent discrete-time channel model, M-ary data symbols are processed in pairs $[\,x[k], x[k+1]\,]$ and transmitted over two antennas according to

$$\mathbf{A}[k] \doteq \begin{array}{c} \left[\begin{array}{cc} x[k] & -x^*[k+1] \\ x[k+1] & x^*[k] \end{array} \right] \begin{array}{l} \longleftarrow \text{Time index } k \\ \longleftarrow \text{Time index } k+1 \end{array} \\ \begin{array}{cc} \uparrow & \uparrow \\ \text{Antenna 1} & \text{Antenna 2} \end{array} \end{array} \tag{1}$$

where $(.)^*$ denotes complex conjugation[1]. Here, focus will be on binary transmission ($M=2$), i.e., $x[k]\in\{\pm 1\}$.

The physical channel is modeled as a frequency-flat block-fading channel, e.g., characterized by a Rayleigh distribution or by a Rician distribution. Moreover, it is assumed that a square-root Nyquist filter is used both at the Tx nodes and at the Rx node (baud-rate sampling is presumed).

Normalization is in the sequel done such that $\delta_1 = 0$ and $\alpha_1 = 1$ for the first transmission path, without loss of generality. For the second transmission path, let $\delta_2 \geq 0$ and $\alpha_2 \leq 1$. The following four scenarios are distinguished:

(i) The Tx nodes apply perfect TA and perfect LA, i.e., $\delta_2 = \delta_1 = 0$ and $\alpha_2 = \alpha_1 = 1$.
(ii) The Tx nodes apply perfect TA, but no or non-perfect LA, i.e., $\delta_2 = \delta_1 = 0$ and $\alpha_2 \doteq \alpha \leq 1$.
(iii) The Tx nodes apply perfect LA, but no or non-perfect TA, i.e., $\delta_2 \doteq \delta \geq 0$ and $\alpha_2 = \alpha_1 = 1$.
(iv) The Tx nodes apply neither perfect TA nor perfect LA.

[1] In this paper, the transposed of the original matrix [4] is used.

The first scenario corresponds to a conventional multiple-antenna system with colocated antennas. In the sequel, focus is on scenario (ii) and on scenario (iii). If neither perfect TA nor perfect LA is applied, the path gain α and the delay δ have *independent* impacts on the system performance and may therefore be treated separately. Accordingly, the last scenario does not yield new insights and is therefore not considered further.

It is assumed in the sequel that for each realization of the fading process, the channel coefficients, i.e., the coefficients of the equivalent discrete-time channel model, are perfectly known at the receiver. If perfect TA is applied (and if the optimum sampling phase is used), the transmission path from Tx node Tx_i ($i=1,2$) to the Rx node can be modeled by a single complex-valued channel coefficient $h_i \doteq a_i \exp(\mathrm{j}\phi_i)$ with $\mathrm{E}\{|h_i|^2\} \doteq \alpha_i$, which is constant over the duration of a complete transmission block ($\mathrm{E}\{.\}$ denotes expectation). In this case, the orthogonal properties of the Alamouti matrix $\mathbf{A}[k]$ may be exploited, and maximum-likelihood detection of the transmitted data symbols $x[k]$ and $x[k+1]$ at the receiver may be performed by a simple matrix-vector multiplication and a subsequent hard decision [4]. However, if the relative propagation delay δ is not compensated, ISI occurs (cf. Section IV) and an appropriate equalizer/detector algorithm is required at the receiver.

To start with, the case of perfect TA is considered.

III. Perfect Timing Advance

If perfect TA and additionally perfect LA is performed, i.e. $\alpha = 1$, the two transmission paths from Tx node Tx_i ($i=1,2$) to the Rx node are characterized by the same average SNR. Assuming Rayleigh fading, an analytical expression for the bit error rate (BER) performance of the distributed Alamouti scheme is given by [12, Ch. 14.4]

$$P_\mathrm{b} = \frac{1}{2}\left[1 - \mu - \frac{\mu}{2}\left(1-\mu^2\right)\right], \quad \mu = \frac{1}{\sqrt{1+\frac{2N_0}{E_\mathrm{s}}}}, \tag{2}$$

where E_s denotes the average symbol energy and N_0 the single-sided noise power density. In order to provide a fair comparison with a (1x1)-system, the overall transmission power of each Tx node has been normalized by the factor 1/2. If no or non-perfect LA is performed ($\alpha < 1$), the two transmission paths will have different average SNRs. In this case, the BER performance of the distributed Alamouti scheme is given by [12, Ch. 14.5]

$$P_\mathrm{b} = \frac{1}{2}\left[\frac{1-\mu}{1-\alpha} + \frac{\alpha\,(1-\mu_\alpha)}{\alpha-1}\right], \quad \mu_\alpha = \frac{1}{\sqrt{1+\frac{2N_0}{\alpha E_\mathrm{s}}}}, \tag{3}$$

again assuming Rayleigh fading. It can be shown that (2) and (3) are equivalent for $\alpha \to 1$.

Fig. 2 illustrates the BER performance of the distributed Alamouti scheme as a function of E_s/N_0 in dB, for different values of α. Simulation results are provided for both Rayleigh fading (solid lines) and Rician fading with a Rice factor of 0 dB (dotted lines). The simulation results have been obtained by means of Monte-Carlo simulation over 10^6 channel realizations. The analytical results for Rayleigh fading according to (2) and (3) are as well included and marked with '+'. As can be seen, the simulative results match the analytical results very well. Note that for $\alpha = 1$ a diversity degree of two is observed – as expected, i.e., for large E_s/N_0 the BER decreases with $1/(E_\mathrm{s}/N_0)^2$. For $\alpha = 0$, however, a diversity degree of

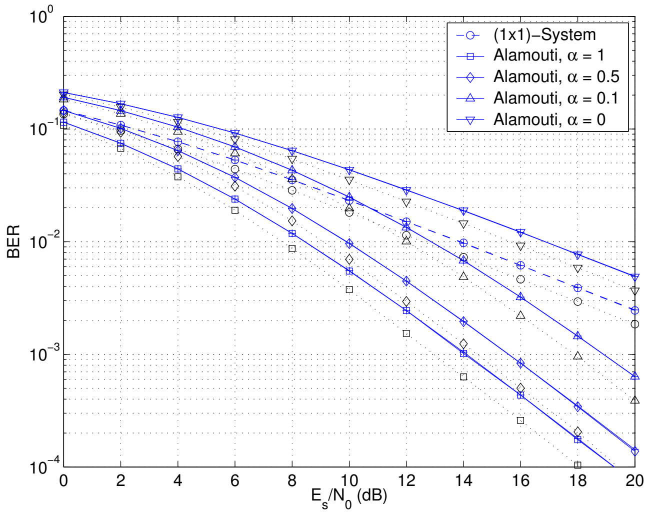

Fig. 2. BER performance of the distributed Alamouti scheme as a function of E_s/N_0 in dB, given different average path gains α for the second transmission path. Solid lines: Rayleigh fading (simulative and analytical results, marked with '+'); dotted lines: Rician fading with Rice factor 0 dB.

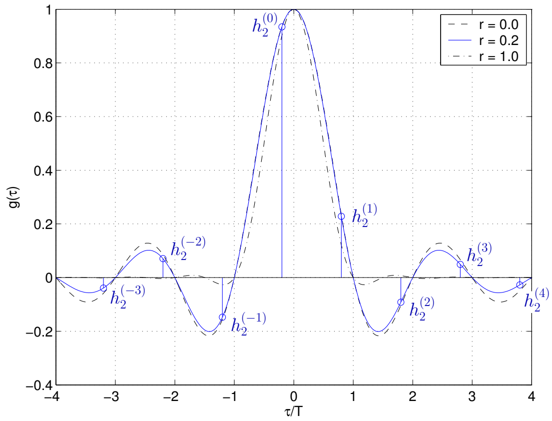

Fig. 3. Example for the ISI caused by the second transmission path, given a relative propagation delay $\delta = T/5$ (T denotes the symbol duration, baud-rate sampling presumed; square-root Nyquist filter with cosine roll-off used at both the Tx nodes and the Rx node, different roll-off factors $0 \leq r \leq 1$ considered).

one results, and a 3 dB-loss with respect to the corresponding (1x1)-system is observed, due to the normalization of the overall transmission power. Given Rician fading, the BER curves are in all cases approximately 1 dB better than the corresponding curves for Rayleigh fading (large E_s/N_0).

IV. Non-Perfect Timing Advance

If the distributed Alamouti scheme is used in conjunction with no or with non-perfect TA, the relative propagation delay δ on the second transmission path ($\mathrm{Tx}_2 \rightarrow \mathrm{Rx}$) is in general greater than zero. Without loss of generality, it is assumed in the sequel that the sampling phase is optimized with respect to the first transmission path. This means that ISI is caused by the second transmission path. Therefore, an equalizer is required at the receiver.

In the sequel, it is assumed that a square-root Nyquist filter $f(\tau)$ with cosine roll-off (roll-off factor r) is used at both the Tx nodes and the Rx node. The overall impulse response of transmitter and receiver is therefore given by $g(\tau) = f(\tau) * f(\tau)$, where the asterisk denotes convolution. In Fig. 3 the occurring ISI is exemplified, showing the channel coefficients $h_2^{(l)}$ that result for the second transmission path, given a roll-off factor of $r = 0.2$ and a delay $\delta = T/5$. Plots for $r = 0$ and $r = 1$ are as well included. In general, given a delay $\delta = \Delta$ with $0 \leq \Delta < 1$, the channel coefficients $h_2^{(l)}$ result as

$$h_2^{(l)} \;=\; \underbrace{c \cdot \frac{\sin(\xi)}{\xi} \, \frac{\cos(r\xi)}{1 - (2r\xi/\pi)^2}}_{\doteq\; g(lT-\Delta)} \cdot a_2 \exp(\mathrm{j}\phi_2)\,, \tag{4}$$

where

$$\xi \;\doteq\; \frac{\pi}{T}\,(lT - \Delta)\,. \tag{5}$$

The normalization factor c is chosen such $\sum_l g(lT-\Delta) = 1$. As earlier, a_2 and ϕ_2 are constant over the duration of a complete transmission block ($\mathrm{E}\{a_2^2\} = \alpha_2 \doteq 1$). It turns out that for $l < -1$ and for $l > 2$ the average powers $\mathrm{E}\{|h_2^{(l)}|^2\}$ are approximately zero for all $0 \leq \Delta < 1$. The transmission path $\mathrm{Tx}_2 \rightarrow \mathrm{Rx}$ is therefore modeled by the channel coefficients

$$\mathbf{h}_2 \;=\; [\, h_2^{(-1)} \; h_2^{(0)} \; h_2^{(1)} \; h_2^{(2)} \,] \tag{6}$$

in the sequel. The dominant channel coefficients are $h_2^{(0)}$ and $h_2^{(1)}$. For delays $\delta = nT + \Delta$, $n > 0$ integer, one obtains

$$\mathbf{h}_2 \;=\; [\, \underbrace{0 \;\cdots\; 0}_{n \text{ zeros}} \; h_2^{(-1)} \; h_2^{(0)} \; h_2^{(1)} \; h_2^{(2)} \,]\,, \tag{7}$$

and for $\delta = 0$ one obtains $\mathbf{h}_2 = [\,0 \;\, a_2 \exp(\mathrm{j}\phi_2) \;\, 0 \;\, 0\,]$. The channel coefficients for the first transmission path are always given by $\mathbf{h}_1 = [\,0 \;\, a_1 \exp(\mathrm{j}\phi_1) \;\, 0 \;\, 0\,]$.

In the sequel, the trellis-based joint equalizer/detector algorithm for the Alamouti scheme in the presence of ISI proposed in an earlier work [8] is briefly recapitulated.

A. Trellis-Based Equalizer/Detector for the Alamouti Scheme

The equalizer/detector has to account for the specific structure of the Alamouti scheme according to (1). This means, standard equalizer algorithms already available for a (1x1)-system are not suitable, and a generalized algorithm is required. It turns out that the received samples should be processed in pairs – corresponding to the transmitter structure, because then the equalizer complexity in terms of the number of trellis states is minimized [8]. To be specific, if the effective channel memory length L is an even number, the number of states for maximum-likelihood sequence estimation (MLSE) resulting for the Alamouti scheme is the *same* as in the corresponding (1x1)-system, namely M^L. If L is an odd number, M^{L+1} trellis states are required. Due to the pairwise processing of the received samples, each trellis segment in the Alamouti trellis spans *two* consecutive time indices k and $k+1$, as opposed to a single time index k in the (1x1)-system. The starting states of the trellis segment for k, $k+1$ are given by all possible K-tuples of M-ary symbol hypotheses $\tilde{x}[\,.\,]$ for the data symbols $x[k-K]$, ..., $x[k-1]$, where $K = L$ for even L and $K = L+1$ for odd L. The target states are given by all possible K-tuples $[\,\tilde{x}[k-K+2], \, \ldots, \, \tilde{x}[k-1]\,, \, \tilde{x}[k]\,, \, \tilde{x}[k+1]\,]$.

In the case of the distributed Alamouti scheme, the effective channel memory length L is in essence determined by the delay

δ occurring on the second transmission path ($\mathrm{Tx}_2 \rightarrow \mathrm{Rx}$). Only if $\delta = 0$, the effective channel memory length is zero (flat fading assumed). Otherwise, for $n > 0$ integer, L is roughly

$$L \approx \begin{cases} n & \text{if} \quad \delta = nT \\ n+2 & \text{if} \quad \delta = nT + \Delta, \quad 0 < \Delta < 1 \end{cases} \tag{8}$$

(cf. (6) and (7)). For MLSE, the metric increment μ_i associated with a certain branch i within the trellis segment for k, $k+1$ is given by

$$\mu_i = |\, y[k] - \tilde{y}_i[k] \,|^2 + |\, y[k+1] - \tilde{y}_i[k+1] \,|^2 \,, \tag{9}$$

where $y[k]$, $y[k+1]$ denote the received samples at time index k and $k+1$, respectively, and $\tilde{y}_i[k]$, $\tilde{y}_i[k+1]$ the corresponding hypotheses resulting from the starting state and the target state of the trellis branch i under consideration. Using (7), the hypotheses $\tilde{y}_i[\,.\,]$ for the branch i are calculated as

$$\begin{aligned} \tilde{y}_i[k] &= h_1^{(0)} \tilde{x}_i[k] \\ &\quad + h_2^{(-1)} \tilde{x}_i^*[k-n] - h_2^{(0)} \tilde{x}_i^*[k+1-n] \\ &\quad + h_2^{(1)} \tilde{x}_i^*[k-2-n] - h_2^{(2)} \tilde{x}_i^*[k-1-n] \,, \\ \tilde{y}_i[k+1] &= h_1^{(0)} \tilde{x}_i[k+1] \\ &\quad - h_2^{(-1)} \tilde{x}_i^*[k+3-n] + h_2^{(0)} \tilde{x}_i^*[k-n] \\ &\quad - h_2^{(1)} \tilde{x}_i^*[k+1-n] + h_2^{(2)} \tilde{x}_i^*[k-2-n] \end{aligned} \tag{10}$$

if $n \geq 0$ is an even integer (and $0 \leq \Delta < 1$). If n is an odd integer, the hypotheses $\tilde{y}_i[\,.\,]$ are calculated according to

$$\begin{aligned} \tilde{y}_i[k] &= h_1^{(0)} \tilde{x}_i[k] \\ &\quad - h_2^{(-1)} \tilde{x}_i^*[k+2-n] + h_2^{(0)} \tilde{x}_i^*[k-1-n] \\ &\quad - h_2^{(1)} \tilde{x}_i^*[k-n] + h_2^{(2)} \tilde{x}_i^*[k-3-n] \,, \\ \tilde{y}_i[k+1] &= h_1^{(0)} \tilde{x}_i[k+1] \\ &\quad + h_2^{(-1)} \tilde{x}_i^*[k+1-n] - h_2^{(0)} \tilde{x}_i^*[k+2-n] \\ &\quad + h_2^{(1)} \tilde{x}_i^*[k-1-n] - h_2^{(2)} \tilde{x}_i^*[k-n] \,. \end{aligned} \tag{11}$$

With growing delay δ, the complexity of the above equalizer/detector soon becomes prohibitive, due to the increased effective channel memory length L. In the following section, a fixed equalizer/detector complexity is considered.

B. Fixed Equalizer/Detector Complexity

Assume an equalizer/detector with a fixed number of $M^{L_{\mathrm{eq}}}$ trellis states, where $L_{\mathrm{eq}} \leq L$. Then, the last $\lambda = (L - L_{\mathrm{eq}})$ channel coefficients of $\mathbf{h}_2$ according to (7) are not taken into account, i.e., they are implicitly set to zero when calculating the hypotheses $\tilde{y}_i[\,.\,]$ according to (10) or (11). This causes residual ISI, which leads to a systematic error in the metric increments μ_i and thus to a performance loss. Fig. 4 shows the average channel power

$$P_{\mathrm{ch}} = \mathrm{E}\{|h_2^{(2-\lambda+1)}|^2\} + \cdots + \mathrm{E}\{|h_2^{(2)}|^2\} \tag{12}$$

discarded by the equalizer/detector as a function of the delay δ (cf. (4)), for the example $L_{\mathrm{eq}} = 4$ and different roll-off factors r. As can be seen, the equalizer/detector is suitable for delays $\delta \leq 3T$, whereas significant residual ISI occurs for larger delays.

In Section IV-D it is shown that an equalizer/detector algorithm of practicable computational complexity can also be derived for larger delays δ.

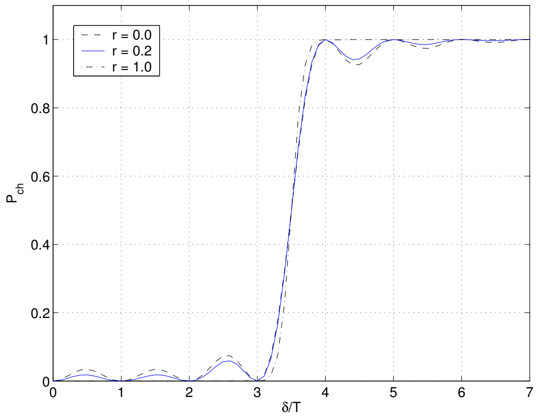

Fig. 4. Average channel power P_{ch} discarded by the equalizer/detector as a function of the delay δ, for the example $L_{\mathrm{eq}} = 4$ and different roll-off factors r.

C. Influence of the Relative Delay on the System Performance

In this section, the influence of the relative propagation delay δ on the system performance is illustrated. This is done by means of simulation results for binary transmission and Rayleigh fading, obtained by Monte-Carlo simulation over 10^6 channel realizations.

Fig. 5 shows simulation results for delays δ that are a multiple of the symbol duration T ($\delta = 0$, T, ..., $6T$), given an equalizer/detector complexity of 2^6 ($L_{\mathrm{eq}} = 6$). On the second transmission path only the channel coefficient $h_2^{(0)}$ is non-zero in this case (cf. (7)), and the roll-off factor r does not have any impact. As can be seen, for delays $\delta = nT$ with $n \geq 2$, the BER performance is very close to the case $\delta = 0$. However, for $\delta = T$ a significant performance loss occurs (about 7 dB at a BER of 10^{-3}). Moreover, for large E_{s}/N_0 the slope of the BER curve corresponds to that of the (1x1)-system, i.e., the diversity advantage is lost. This performance loss is due to the fact that poor distance properties arise for $\delta = T$. From (10) and (11) it can be seen that there is a considerable difference between the case $\delta = T$ and the cases $\delta = nT$, $n \geq 2$. For $\delta = T$, the received samples $y[k]$ and $y[k+1]$ are determined by just three different transmitted data symbols, namely by $x[k]$, $x[k+1]$, and $x[k-2]$ (cf. (11), $n \doteq 1$), whereas for $\delta = nT$ with $n \geq 2$, $y[k]$ and $y[k+1]$ are always determined by four different transmitted symbols.

Fig. 6 shows simulation results for arbitrary delays δ between $\delta = 0$ and $\delta = 6T$ and $E_{\mathrm{s}}/N_0 = 20$ dB, given different roll-off factors r and an equalizer/detector with $L_{\mathrm{eq}} = 4$ and $L_{\mathrm{eq}} = 6$, respectively. For delays $\delta > 2T$, the BER performance is close to the case $\delta = 0$, provided that the complexity of the equalizer/detector is sufficiently large (the loss in E_{s}/N_0 is 0.5 dB and less). For the equalizer/detector with $L_{\mathrm{eq}} = 4$ a significant performance loss occurs if $\delta > 3T$, as expected (cf. Fig. 4).

The performance loss occurring for $\delta = T$ may be circumvented even if perfect knowledge of the delay δ is not available at the Tx nodes. It might still be known, which of the two transmission paths is associated with the larger propagation delay. In this case, the Tx nodes may perform a coarse timing adaptation, by delaying the corresponding signal by two of more symbol durations. The equalizer/detector complexity at the receiver must be chosen sufficiently large, however.

In the sequel, it is shown that an equalizer/detector algorithm of practicable computational complexity can also be derived for large delays.

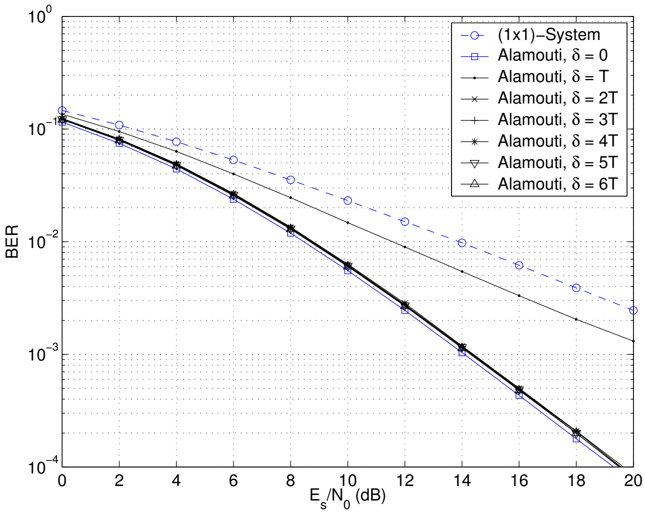

Fig. 5. BER performance of the distributed Alamouti scheme as a function of E_{s}/N_0 in dB, given relative propagation delays δ that are a multiple of the symbol duration T ($\delta = 0,\ T,\ \dots, 6T$); simulative results for Rayleigh fading and $L_{\mathrm{eq}} = 6$.

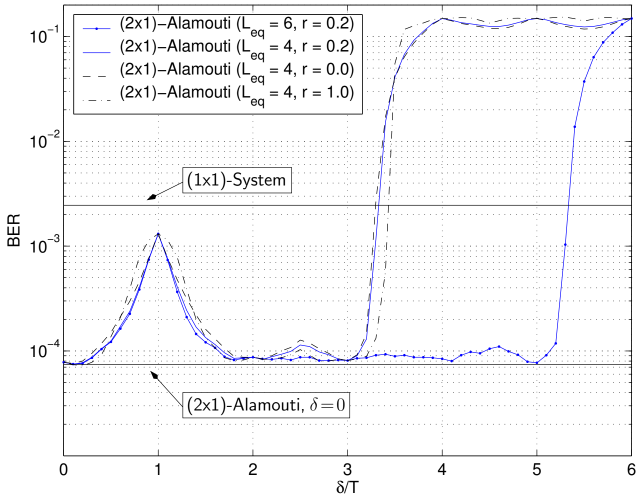

Fig. 6. BER performance of the distributed Alamouti scheme as a function of the relative propagation delay δ, given different roll-off factors r and different equalizer/detector complexities; simulative results for Rayleigh fading and $E_{\mathrm{s}}/N_0 = 20$ dB.

D. Large Relative Propagation Delays

According to (8), the effective channel memory length L increases with growing n. However, revisiting (10) and (11), one observes that the overall number of symbol hypotheses $\tilde{x}[\,.\,]$ required to calculate the hypotheses for $y[k]$ and $y[k+1]$ does *not* depend on the delay δ. This fact may be exploited in order to significantly reduce the complexity of the equalizer/detector algorithm, without causing any performance loss. Given a delay $\delta = nT + \Delta,\ 0 < \Delta < 1$, a metric increment μ_i associated with a certain trellis branch i is determined by altogether seven different symbol hypotheses $\tilde{x}[\,.\,]$ (cf. (10) and (11)). Therefore, although each trellis segment contains $M^{n+2}M^2$ branches if n is an even number and $M^{n+3}M^2$ branches if n is an odd number, there are altogether only M^7 *different* metric increments. By avoiding to compute the same metric increment several times, the computational complexity is reduced to a degree still tractable in practice, at least for binary transmission. However, the storage requirements are the same as in the full-complexity algorithm (Section IV-A), since the number of trellis states is not reduced.

The above reasoning corresponds to the concept of trellis-based equalization for *sparse* wireless communication channels [9]. Sparse channels are channels with a large effective memory length, but only a few significant channel coefficients. Given a sparse channel, two different approaches are proposed in [9] and [10] to reduce both the computational complexity and the storage requirements for trellis-based equalization. In the case of the distributed Alamouti scheme, however, it turned out that the approach in [9] does *not* lead to a reduced complexity. Moreover, it turned out that the approach in [10] cannot be applied to the case of the distributed Alamouti scheme, because this approach requires a sparse channel with a distinct structure in the time domain, which is not met.

V. Conclusions

In this paper, the application of a distributed Alamouti scheme has been considered, and a key challenge has been pointed out that is due to the distributed nature of the scheme: Since the distances between the two transmitting nodes and the receiving node are typically different, the transmitted signals are subject to different propagation delays as well as to different average path gains. By means of simulative and analytical results, it has been shown that both effects can cause a significant performance loss, unless appropriate (transmitter-sided and/or receiver-sided) counter measures are applied. Specifically, the use of a trellis-based joint equalizer/detector algorithm for the Alamouti scheme in the presence of intersymbol interference has been investigated.

Acknowledgment: The authors would like to thank Ingmar Land (ICT, University of Kiel) for fruitful discussions.

References

[1] D. Gesbert, M. Shafi, D. Shiu, P. J. Smith, and A. Naguib, "From theory to practice: An overview of MIMO space-time coded wireless systems," *IEEE J. Select. Areas Commun.*, vol. 21, no. 3, pp. 281-302, Apr. 2003.
[2] A. Wittneben, "Basestation modulation diversity for digital SIMULCAST," in *Proc. IEEE Veh. Technol. Conf. (VTC'91)*, 1991, pp. 848-853.
[3] J. N. Laneman and G. W. Wornell, "Distributed space-time-coded protocols for exploiting cooperative diversity in wireless networks," *IEEE Trans. Inform. Theory*, vol. 49, no. 10, pp. 2415-2425, Oct. 2003.
[4] S. M. Alamouti, "A simple transmit diversity technique for wireless communications," *IEEE J. Select. Areas Commun.*, vol. 16, no. 8, pp. 1451-1458, Oct. 1998.
[5] V. Tarokh, H. Jafarkhani, and A. R. Calderbank, "Space-time block codes from orthogonal designs," *IEEE Trans. Inform. Theory*, vol. 45, no. 5, pp. 1456-1467, June 1999.
[6] X.-B. Liang and X.-G. Xia, "On the nonexistence of rate-one generalized complex orthogonal designs," *IEEE Trans. Inform. Theory*, vol. 49, no. 11, pp. 2984-2989, Nov. 2003.
[7] Z. Chen, J. Yuan, B. Vucetic, and Z. Zhou, "Performance of Alamouti scheme with transmit antenna selection," *IEE Electron. Lett.*, vol. 39, no. 23, pp. 1666-1668, Nov. 2003.
[8] J. Mietzner, P. A. Hoeher, and M. Sandell, "Compatible improvement of the GSM/EDGE system by means of space-time coding techniques," *IEEE Trans. Wireless Commun.*, vol. 2, no. 4, pp. 690-702, Jul. 2003.
[9] N. Benvenuto and R. Marchesani, "The Viterbi algorithm for sparse channels," *IEEE Trans. Commun.*, vol. 44, no. 3, pp. 287-289, Mar. 1996.
[10] N. C. McGinty, R. A. Kennedy, and P. Hoeher, "Parallel trellis Viterbi algorithm for sparse channels," *IEEE Commun. Lett.*, vol. 2, no. 5, pp. 143-145, May 1998.
[11] R. Steele and L. Hanzo, *Mobile Radio Communications.* 2nd ed., Chichester: John Wiley & Sons, Ltd., 1999.
[12] J. G. Proakis, *Digital Communications.* 4th ed., New York: McGraw-Hill, 2001.